

Critical exponents and scaling invariance in the absence of a critical point

N. Saratz¹, D. A. Zanin¹, U. Ramsperger¹, S. A. Cannas², D. Pescia¹, and A. Vindigni^{1*}

¹*Laboratorium für Festkörperphysik, Eidgenössische Technische Hochschule Zürich, CH-8093 Zürich, Switzerland and*

²*Facultad de Matemática, Astronomía y Física (IFEG-CONICET),*

Universidad Nacional de Córdoba, Ciudad Universitaria, 5000 Córdoba, Argentina

(Dated: May 27, 2022)

The paramagnetic-to-ferromagnetic phase transition is believed to proceed through a critical point, at which power laws and scaling invariance, associated with the existence of one diverging characteristic length scale – the so called correlation length – appear. We indeed observe power laws and scaling behavior over extraordinarily many decades of the suitable scaling variables at the paramagnetic-to-ferromagnetic phase transition in ultrathin Fe films. However, we find that, when the putative critical point is approached, the singular behavior of thermodynamic quantities transforms into an analytic one: the critical point does not exist, it is replaced by a more complex phase involving domains of opposite magnetization, below as well as *above* the putative critical temperature. All essential experimental results are reproduced by Monte-Carlo simulations in which, alongside the familiar exchange coupling, the competing dipole-dipole interaction is taken into account. Our results imply that a scaling behavior of macroscopic thermodynamic quantities is not necessarily a signature for an underlying second-order phase transition and that the paramagnetic-to-ferromagnetic phase transition proceeds, very likely, in the presence of at least two long spatial scales: the correlation length and the size of magnetic domains.

Keywords: Phase transitions, Scaling hypothesis, Avoided critical point

I. INTRODUCTION

Our understanding of the ferromagnetic phase transition foresees the appearance of a finite, spatially uniform spontaneous (i.e. occurring in zero applied magnetic field) magnetization as the temperature is lowered below a well-defined critical (Curie) temperature¹. Strictly speaking, however, a finite three-dimensional body (i.e. a body extending over sufficiently large but *finite* lengths in all three spatial directions) lacks a finite uniform magnetization at any temperature², as a result of the dipole-dipole interaction, which, albeit weak, frustrates the tendency to ferromagnetism inherent to the exchange interaction^{3,4}. Thus, the dipole-dipole interaction leads necessarily to a situation of “avoided critical point”⁵, where the phase transition proceeds via a yet not fully elucidated and probably not universal mechanism^{5–10,40}. At present, both the theoretical and experimental behavior of the various thermodynamic quantities in the vicinity of such an avoided critical point are uncertain. Here we demonstrate, on one side, the validity of conventional notions like critical exponents and scaling hypothesis¹ in the vicinity of such an avoided critical point, implying the existence of a correlation length governing the phase transition. On the other side, we also establish that, when the putative critical point is *approached*, the non-analytic behavior transforms into an analytic one. Simultaneously, we observe that the paramagnetic-to-ferromagnetic phase transition proceeds within a background of spatially nonuniform magnetization. This observation implies that the typical period of modulation – established by the competition between exchange and dipole-dipole interaction and characterizing the phase with nonuniform magnetization – persists below as well as above the putative critical temperature, alongside the correlation length.

II. STRATEGY

The paramagnetic-to-ferromagnetic phase transition investigated in this work occurs in ultrathin Fe films grown at room temperature by molecular-beam epitaxy onto the (001) surface of a Cu single crystal (see Ref. 12 for details). The system has macroscopic lengths within a plane but finite thickness perpendicular to the plane (typically between 1.6 and 2.0 atomic monolayers (ML)). It is magnetized perpendicularly to the plane, so that it has the right symmetry to realize the famous Onsager critical point³⁷ of the two-dimensional (2D) Ising model. However, as shown in Ref. 14, it also suffers the very same frustration foreseen for finite three-dimensional bodies so that the paramagnetic-to-ferromagnetic phase transition is associated with the appearance of stripes and/or bubble domains of opposite magnetization rather than with the formation of a spatially uniform spontaneous magnetization^{7,15–24}. Accordingly, the transition falls into the category of transitions with “avoided critical point”. We have followed three strategies: On one side an experimental one, consisting in performing magneto-optical Kerr effect (MOKE)²⁵ measurements of the macroscopic, spatially averaged magnetization as a function of temperature T and external magnetic field H applied perpendicularly to the film. Technically speaking, MOKE measures a signal which is *proportional* to the average magnetization²⁵. Here we use the character “ M ” to identify the measured quantity, which is accordingly given in arbitrary units. In a second step, the measurement of macroscopic thermodynamic quantities was complemented with spatially resolved magnetic imaging – performed with SEMPA¹⁸ – aimed at measuring the evolution of the *local* magnetization during the phase transition, with submicrometer spatial resolution. The complementary use of MOKE and SEMPA microscopy to

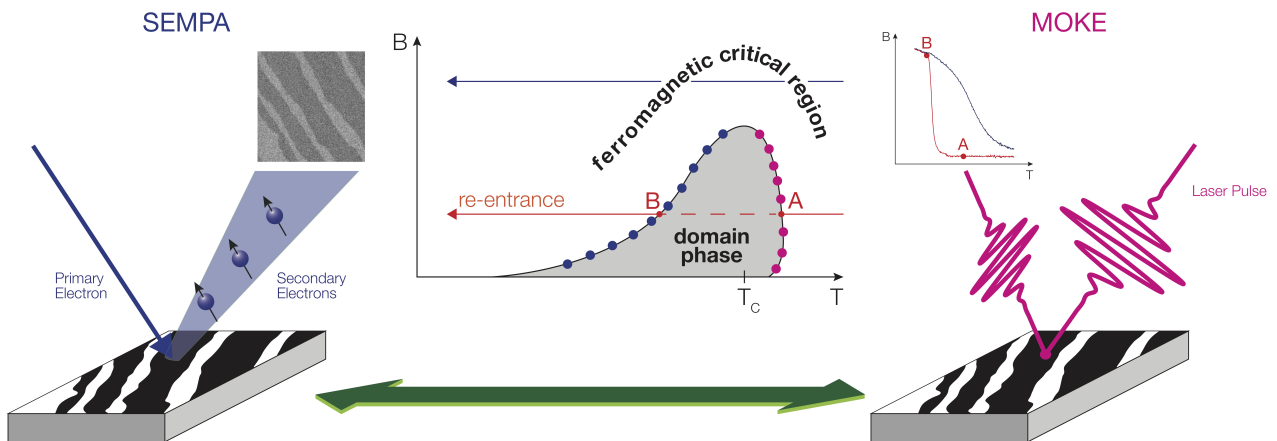


FIG. 1: Sketch representing the complementary use of MOKE and SEMPA techniques to determine the phase diagram of Fe/Cu(001) films. SEMPA allows defining the phase boundaries by direct visualization of the domain pattern realized for a given pair of values of T and H (e.g., blue dots in the pictorial phase diagram); this approach can, however, be applied as long as the time needed to scan a whole image (\sim minutes) is faster than the typical timescale over which domains move. As the putative T_C is approached, domains become mobile and the contrast is lost. The information extracted from SEMPA imaging was complemented with MOKE measurements of the *global* magnetization, in which a lapse of time in the range of seconds was used to sweep a full magnetization curve at constant T . Fuchsia dots exemplify a boundary between the uniform phase and the domain-patterned phase that can be defined through the analysis of MOKE data described in this work. The blue and the orange paths indicated in the phase diagram produce the two types of magnetization curves reported in the inset on the right and described in section III.A.

define the phase diagram of the Fe films investigated in this work is pictorially sketched in Fig.1. Finally, we explored the possibility of realizing the scaling hypothesis in Monte-Carlo simulations of a 2D Ising model, with spins on a lattice and interacting via the familiar exchange interaction – which promotes ferromagnetic order – and dipolar interaction. The latter, albeit weak, is long ranged and in films magnetized perpendicularly to the plane frustrates the tendency to ferromagnetism. In the presence of the dipolar interaction, it is not a priori clear whether any scaling behavior – explicit in the 2D Ising model with pure exchange interaction – is left behind, nor in which region of the (T, H) parameter space such scaling might be found.

III. RESULTS

A. Scaling plots

Magnetization curves $M(T, H)$ are plotted as a $M(T)$ -family of isochoamps in Fig.2. The magnetic field was swept with a frequency varying between 10^{-1} and 1 Hz. $M(H)$ -curves measured at fixed temperature within this range of frequencies coincide: we assume that we are observing properties related to thermodynamic equilibrium. At higher frequencies we have detected a substantial dynamical component and the results of these studies will be reported in a separate paper. A color code, indicated along the vertical bar, is used for the values of H . We distinguish two extreme sets of $M(T)$ -curves. On the

right-hand side those corresponding to larger values of H , taken in a state of uniform magnetization. They show the familiar behavior of $M(T)$ -curves separating out with increasing magnetic field and are suggestive of a conventional underlying critical point becoming more and more “avoided” with increasing applied magnetic field (this is an example of trivially “avoided critical point”⁵). On the left-hand side the family of curves corresponding to low H : while the temperature is increased the average magnetization abruptly drops to almost zero as the system enters the state of static modulated order, observed directly with SEMPA (not reported here). Those images indicate that the magnetization within the domains is still large and therefore the vanishing of M (*global* magnetization) below $\simeq 300$ K for small applied fields is entirely due to the cancellation of finite opposite values of the local magnetization within the domains. We point out, however, that our distinction between “high” and “low” magnetic field curves is based on our imaging of the spatial distribution of the magnetization: the macroscopic thermodynamic quantity $M(T, H)$ itself does not contain, at first glance, any specific information which could be used to classify the set of $M(T)$ -curves.

The scaling hypothesis¹ states that the equation of state $M = M(T, H)$ can be simplified to a one variable relation $\tilde{M} = \tilde{M}(\tilde{\tau})$, provided the rescaled variables $\tilde{M} := M/H^{1/\delta}$ and $\tilde{\tau} := \tau/H^{\delta\beta}$ are used, $\tau = (T - T_C)/T_C$ being the so called reduced temperature. In conventional ferromagnets T_C is the critical temperature at which, e.g., the *critical isochoamp* (order parameter) $M(T, H = 0)$ vanishes. The critical exponent β is defined via the

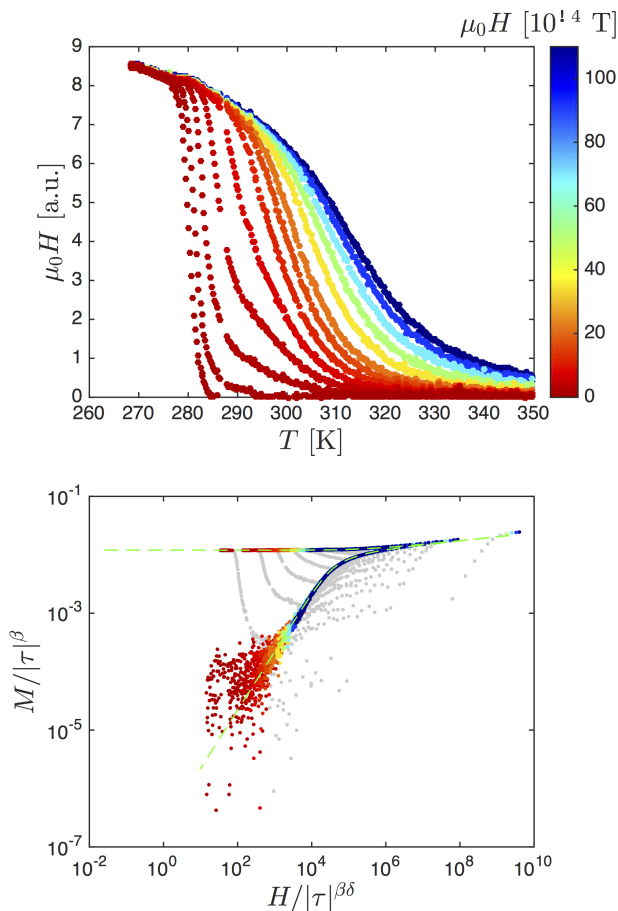


FIG. 2: Top: family of experimental $M(T)$ -isochamps (about 10^5 experimental data points). The film thickness is about 1.75 ML. The color code used for the magnetic field H is given along the vertical bar. Up to T^* static domains of opposite perpendicular magnetization are observed. Bottom: Scaling plot $M/|\tau|^\beta$ versus $H/|\tau|^{\beta\delta}$. The dashed green line represents the numerical scaling function, taken from Ref. 27.

asymptotic behavior of the critical isochamp near T_C , i.e. $M(T, H = 0) \sim (-\tau)^\beta$. In our system this curve does not exist because domains form spontaneously as soon as some sizable magnetization develops locally, leading to cancellation of the *global* magnetization. As a consequence, T_C cannot be located in a standard way, nor can β be determined directly. The critical exponent δ is defined via the asymptotic behavior of the *critical isotherm* $M(T_C, H) \sim H^{1/\delta}$, which – strictly speaking – does not exist either. However, the conventional lore of scaling (Ref. 1, p.485) in the critical or near critical region indicates practical ways to extrapolate values for T_C , β and δ using experimental M -data originating within the high-temperature, non-zero field region of the parameter space, as discussed in Appendices A and B.

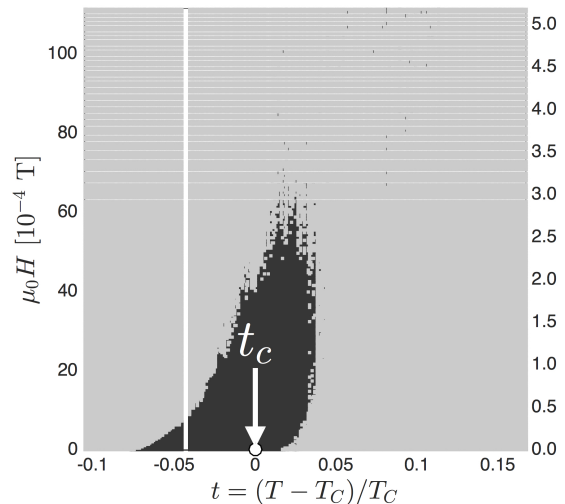


FIG. 3: The same experimental data points are transferred within the (T, H) -parameter space. t_c corresponds to the putative critical temperature used for building the variable τ . The scale on the vertical right hand side gives the values of the magnetic field $\mu_0 \cdot H$ in units of the saturation magnetization of Fe, $\mu_0 \cdot \mathcal{M}_S = 2.16$ T.

B. Phase diagram

Using the values of T_C , β and δ determined experimentally, the data of $M(T, H)$ can be represented in a scaling plot $M/|\tau|^\beta$ versus $H/|\tau|^{\beta\delta}$: The data points that collapse onto the same master curve obey the equation of state of a conventional ferromagnet in the vicinity of T_C . Therefore, “collapsed” and “non-collapsed” points can be reported in the proper location of the (T, H) plane to define the phase diagram. In the scaling plot of Fig.2 (bottom), locations with higher density of data points can be recognized by inspection. Using an ad-hoc software, we marked the low-density points – which we consider as “non-collapsed” – in gray, while the high-density points – which we consider as “collapsed” – were left in their original color (vertical bar in Fig.2). The gray (non-collapsed) data and the black (collapsed) ones are subsequently transferred into their place in the (T, H) plane, Fig.3, where they appear inside, respectively outside, a bell-shaped region marked in gray. To represent the phase diagram in Fig.3 the variable $t := (T - T_C)/T_C$ is used. Notice that many reddish color-coded points appear in the lower left-hand section of the scaling plot Fig.2 (bottom). They correspond to high temperatures and low applied magnetic fields and they are scattered because of noise, resulting in a small density. Despite this, we consider them as “collapsed”, because they are spread along the continuation of the scaling function of the 2D Ising model (the dashed line in Fig.2 (bottom)). The bell-shaped region starts on the left with the boundary line marking the transition from (static) modulated-to-uniform phase, recorded by direct SEMPA imaging of

the spatial distribution of the magnetization. It continues beyond the range of temperature and magnetic fields where a static modulation of order is observed and *even beyond* $t = 0$, that is above T_C . Evidently, the static magnetic domains¹⁷ imaged with SEMPA represent only a small portion of the ferromagnetic transition.

Remarkably, the singular behavior of $M = M(T, H)$ expected for a conventional ferromagnet while T_C is approached gives way to an analytic behavior within the “gray zone”. In particular, the M versus H dependence for low magnetic fields is perfectly linear within the “gray” zone, i.e. at sufficiently low magnetic fields a singular behavior, characterized by some non-linear M versus H relationship, does not develop. It appears, therefore, that the non-analytic behavior is precisely suppressed when the putative critical point is approached.

C. Griffiths-Widom representation

An alternative way with respect to Fig.2 (bottom) to express the equation of state of a ferromagnet is the Griffiths-Widom representation³⁹:

$$\frac{H}{M^\delta} = h(x) \quad (1)$$

with $x = \tau/M^{1/\beta}$. In Fig.4 the same data points shown in Fig.2 (bottom) are plotted in this representation with

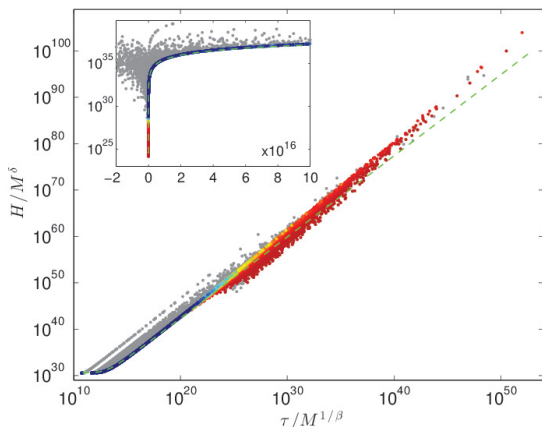


FIG. 4: Scaling plot in the Griffiths-Widom representation H/M^δ vs $x = \tau/M^{1/\beta}$. Data and color codes are the same as in Fig.2. The scale is log-log in the main panel and log-linear in the inset. The green dashed line represents the theoretical scaling function $h(x)$ given in Ref. 27 for the 2D Ising model (shifted by non-universal, constant scaling factors); note that collapsed data points overlap to this line throughout the range $-6 \cdot 10^{12} \lesssim x \lesssim 10^{23}$. The slight deviations for $x > 10^{40}$ are due to the experimental value of the exponent γ being slightly different from the one expected for the 2D Ising (remember that γ is the slope of the graph of Fig.4 for very large values of x).

the same color coding. Particularly clear is how gray points deviate from scaling for the data plotted in the inset ($-2 \cdot 10^{16} \leq x \leq 10^{17}$). In the main frame the non-collapsed, gray points decorate the colored *line* of clearly collapsed points up to $x \sim 10^{23}$. For larger values of x , the main line broadens as well: these are the high temperature, low-field “noisy” data points already discussed in relation to Fig.2. In the Griffiths-Widom representation data collapsing is realized over **forty** orders of magnitude with respect to the x -variable and **eighty** orders of magnitude with respect to the variable H/M^δ . The theoretical scaling function $h(x)$ given in Ref. 27 for the unfrustrated 2D Ising model is plotted as a green dashed line. Colored, collapsed points follow this curve very well up to $x \lesssim 10^{23}$ (note the remarkable agreement in the inset).

D. Monte-Carlo simulations

We consider the Hamiltonian²⁴

$$\mathcal{H} = -J \sum_{\langle i,j \rangle} S_i S_j + g \sum_{(i,j)} \frac{S_i S_j}{r_{ij}^3} + h \sum_i S_i \quad (2)$$

where the spins $S_i = \pm 1$ are defined on a square lattice with $N = L_x \times L_y$ sites and periodic boundary conditions (Ewald sums technique was used to handle them). The first term in Eq. (2) represents the short-range exchange interaction (the sum runs over all pairs of nearest-neighboring sites). The second term represents the long-range dipolar interaction in the Ising limit, the corresponding sum running over *all* pairs of distinct sites on the lattice. The third term represents the Zeeman energy. The Hamiltonian in Eq. (2) is far from describing ultrathin Fe films on Cu(100) in detail. However, it is considered to build a model Hamiltonian capturing realistically competing interactions and the avoided critical point. Accordingly, it has been found to display a variety of modulated phases^{22–24,28} within some region of the (T, h) parameter space, even for those moderate values of the ratio J/g where Monte-Carlo simulations are practicable²⁹. In this particular study we have explored the phase diagram outside this region, with the aim of searching for some residual scaling behavior. In a first step we have determined a limiting field h_c above which the system is in a spatially uniform state, within the temperature range considered by the simulation. h_c was determined from the behavior of the average spin polarization $m := (\sum_i \langle S_i \rangle)/N$ as a function of temperature for fixed values of h , according to a zero-field-cooled–field-cooled (ZFC-FC) protocol³⁰. In a second step we have computed isochamps during the heating part of the ZFC-FC cycle, shown on the top of Fig.5 for $J/g = 10$ and $h_c/g = 0.32 \pm 0.02$. The spreading of the isochamps with different values of the magnetic field is similar to the experimental one reported in the top of Fig.2. In a third step we attempted scaling plots, trying to bring

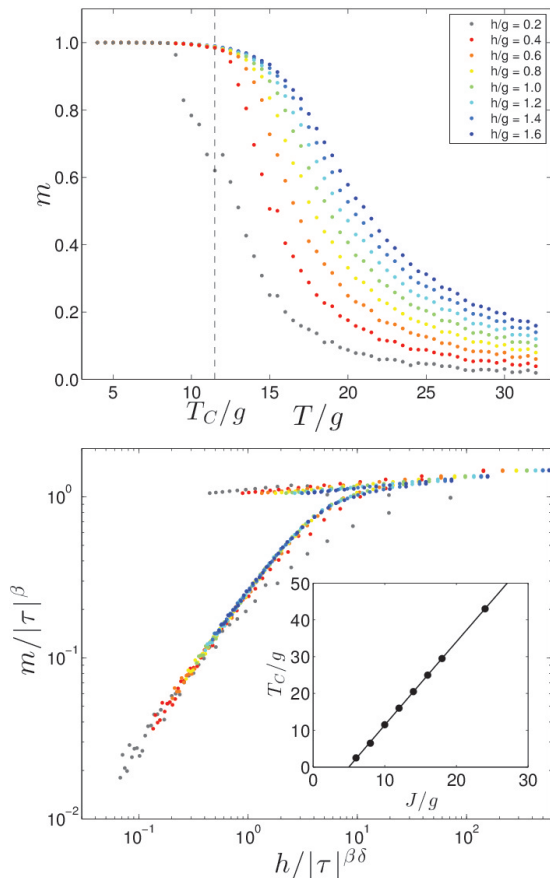


FIG. 5: Monte-Carlo simulations. A family of $m(T)$ -isochamps (top), computed for $J/g = 10$, $L_x = L_y = 120$ and different values of the magnetic field h , collapses onto one single scaling function (bottom) when the magnetic field exceeds the critical value for entering a spatially uniform state of magnetization. The non-collapsed data points correspond to a magnetic field below the threshold. Some simulations taking $L_x = L_y = 200$ were also run to check for possible finite-size effects. The inset at the bottom shows the characteristic temperature T_C , used for optimize data collapsing in the Monte-Carlo scaling plots, as a function of J/g .

the isochamps to collapse onto one single curve. It turned out that collapsing could be indeed realized for $h > h_c$ (colored in the bottom of Fig.5) and a significant departure from collapsing was observed for $h < h_c$ (gray points corresponding to $h/g = 0.2$), i.e. inside the region of the phase diagram where nonuniform magnetization appears. For building the scaling plots of Fig.5 we used the known 2D Ising critical exponents, but the value for the putative critical temperature T_C , required to build the reduced temperature τ , cannot be read out in an obvious way from the set of isochamps of Fig.5. We found, for a practicable set of J/g values, that the best data collapse could be realized assuming a transition temperature given in the inset of Fig.5 (bottom) as a function of J/g . Remarkable about this temperature is that it can

be expressed as the transition temperature for the “pure” 2D Ising model subtracted by a value which corresponds to about $11.2g$ (see Inset of Fig.5 (bottom)). We recall that, within a simple mean-field approach, the presence of the dipolar interaction in a uniformly magnetized state reduces the transition temperature by an amount corresponding to about $4\pi g!$ The picture emerging from Fig.5 is in line with the experimental outcome and underlines the realization of scaling and power laws in a situation where the critical point is avoided.

IV. DISCUSSION

The familiar description of a second-order phase transition foresees that at sufficiently large temperatures T the free-energy density $F(\mathcal{M})$ in the variable \mathcal{M} (average magnetization) has a minimum at $\mathcal{M} = 0$ (Fig.6, top). When the temperature is lowered below a

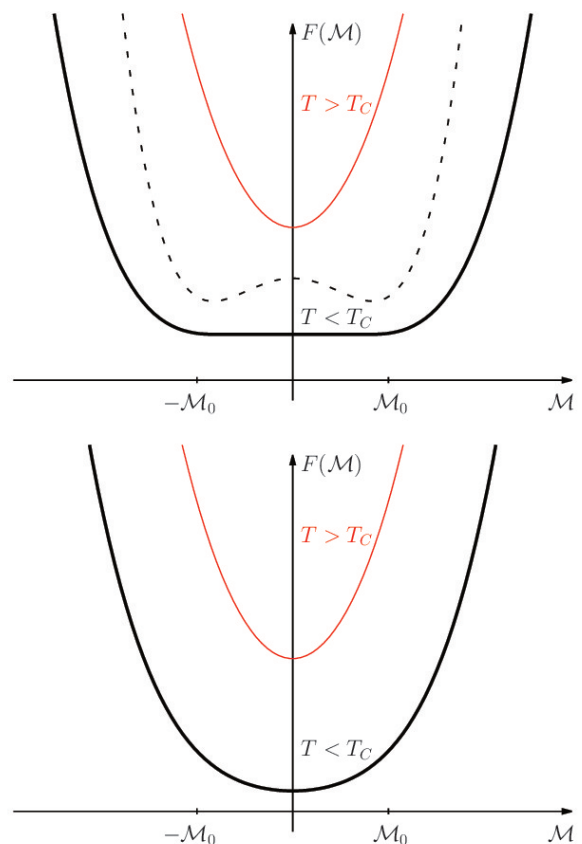


FIG. 6: Top: The Free energy density $F(\mathcal{M})$ for a ferromagnet at T larger than the Curie temperature T_C (thin solid line) and T below T_C (thick solid line). Notice that the flat portion is slightly modified into two flat minima at $\pm \mathcal{M}_0(T)$ if the three dimensional body is large but finite (dashed line)³¹. Bottom: in the presence of the dipolar interaction, the flat portion (the two minima) changes into one single minimum at $\mathcal{M} = 0$.

critical value T_C , the graph of $F(\mathcal{M})$ acquires a flat portion (Fig.6, top) between two limiting values $\pm\mathcal{M}_0(T)$ defining a situation of spontaneously broken symmetry with spatially uniform magnetization $\pm\mathcal{M}_0(T)$. The present paper is in contrast to this picture because it finds that the flat portion is replaced by a minimum of $F(\mathcal{M})$ at $\mathcal{M} = 0$ for *any* temperature (Fig.6, bottom). Notice that we are not the first to point out the difficulty of translating the familiar description of second-order phase transitions¹ to the paramagnetic-to-ferromagnetic transition^{2,3}. But the present results pinpoint some essential elements of the “gray zone” replacing the critical point which were not recognized explicitly yet: *i*) the recovery of the familiar properties of scaling and power laws, albeit *outside* the gray zone and *ii*) the persistence *above* the putative critical temperature of the phase of the magnetic-domain patterns, accessible to spin-sensitive scanning probe techniques *only* below T_C and when domains are static (on the time scale of a specific scanning-probe experiment).

It is important to mention at this point the vast literature^{32,33} describing the cross-over from the exchange controlled criticality to the dipolar-controlled criticality within a *very narrow* temperature range in the vicinity of the critical point. Notice that the cross-over considered in this literature *preserves* the critical point (albeit with slightly modified critical exponents), in contrast to our observations. However, the cross-over scenario refers to a situation of uniform spontaneous magnetization which is actually forbidden for finite three-dimensional bodies. We can, in principle, envisage special situations where a uniform magnetization is possible, such as the infinite-volume limit underlying the cross-over scenarios^{32,33}, but also an inefficient domain nucleation that keeps the body in a metastable state of uniform magnetization, or some very particular shapes (not covered by Ref. 2) which energetically penalize the formation of domains. However, the true absence of any domain, both below as well as *above* the putative critical point, must be verified specifically³⁴, as these situations must be regarded as exceptional while the rule is rather a “gray zone”, i.e. an avoided critical point. Unfortunately, it is very difficult to establish, on the base of experimental and theoretical data related to macroscopic thermodynamic quantities alone, the extent of the gray zone³⁵.

In summary, the recovering of the scaling hypothesis outside the “gray region” means, on one side, that scaling properties and critical exponents, referring to macroscopic thermodynamic quantities, are not necessarily a proof of the existence of a critical point. On the other side, their emergence in a situation of avoided criticality, where the phase transition actually might even be a purely dynamical one⁴⁰, sets some well-defined boundaries on future realistic models of the ferromagnetic phase transition (and of second-order phase transitions in general). These models will have to take into account the presence of (at least) two mesoscopic spatial scales: the correlation length, whose divergence

at the putative critical point is an essential ingredient for the current understanding of critical phenomena, *and* the dipolar-induced period of modulation characterizing the phase with domain patterns.

Acknowledgments – We thank Thomas Bähler for technical assistance, G. M. Graf, A. Giuliani, O. V. Billoni and S. Ruffo for helpful discussions as well as the Swiss National Science Foundation, ETH Zurich, and CON-ICET (Argentina) for financial support.

Appendix A: Experimental determination of T_C

One useful property of a conventional second-order phase transition is that the plot of the magnetic susceptibility $\chi(T, H) = \partial M(T, H)/\partial H$ as a function of the temperature has a maximum at a temperature $T_{max}(H)$

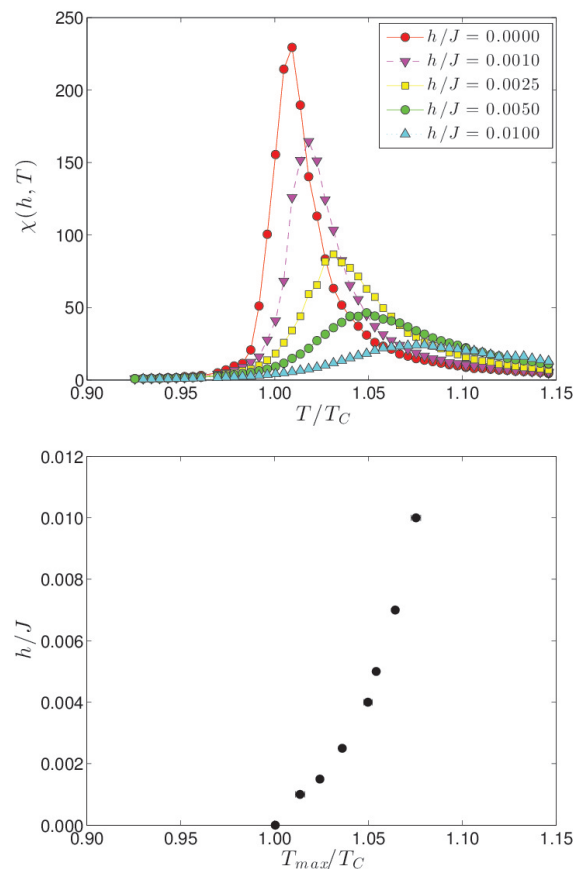


FIG. 7: Monte-Carlo simulations for the pure 2D Ising model. Left: Plot of the magnetic susceptibility $\chi(T, h) = \partial m/\partial h$ as a function of T/T_C for a lattice of linear size $L_x = L_y = 120$; we recall that $T_C = 2.269 J$, assuming $k_B = 1^{37}$; the selected values of h/J are given in the figure legend. Right: h/J versus $T_{max}(h)/T_C$; for each field, the value of $T_{max}(h)$ was extrapolated with finite-size scaling using lattices of size $L_x = L_y = 48, 64, 96, 128$ and 200 .

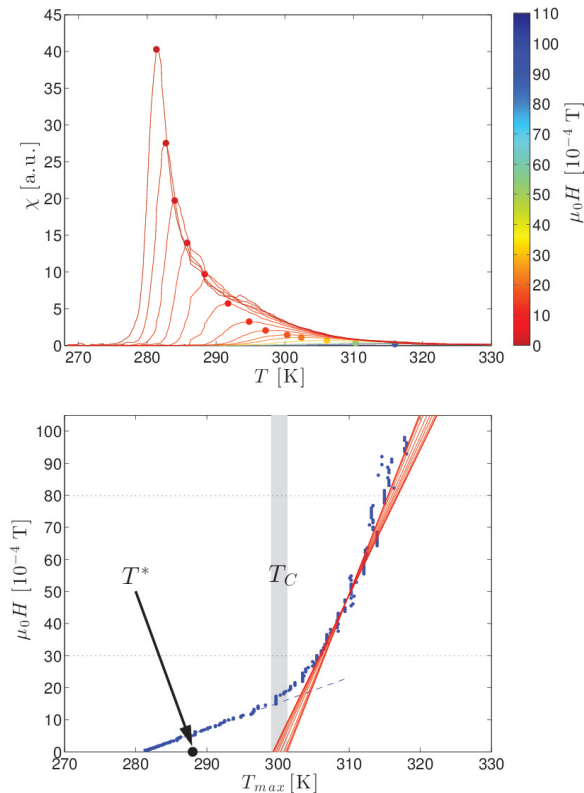


FIG. 8: Top: Plot of the magnetic susceptibility $\chi(T, H) = \partial M(T, H)/\partial H$ of Fe/Cu(001) films as a function of temperature obtained as described in the text. Different colors correspond to different applied fields (see color map on the right). Bottom: Plot of H vs $T_{max}(H)$ obtained from the experimental susceptibility as described in the text; the blue dashed line is a guide to the eye for the maxima marking the re-entrant transition from the patterned to the uniform phase; linear fittings used to determine T_C are drawn as red lines; horizontal dotted lines indicate the region where fittings were performed; the shadowed vertical stripe corresponds to the estimate of $T_C = 300 \pm 1$ K; the temperature T^* above which SEMPA images become contrastless is also indicated.

that approaches T_C as H approaches zero³⁶. Figure 7 (top) shows the susceptibility $\chi(T, H)$ of the “pure” (i.e. without dipolar interactions) 2D Ising model computed by means of Monte-Carlo simulations. For any $H \neq 0$ the maximum value of $\chi(T, H)$ is finite but – as expected – it is higher the weaker the fields are. Notice that the true approach of $T_{max}(H)$ to T_C may not necessarily be linear in H , as pointed out in Ref. 36, but our numerical simulations (bottom of Fig.7) show that a linear extrapolation of T_{max} toward $H = 0$ gives a fairly accurate estimate of T_C .

From the experimental data we obtained the $\chi(T, H)$ by first treating the raw $M(T, H)$ data with a Savitzky-Golay finite-impulse-response smoothing filter implemented in MATLAB. After filtering, the derivative $\chi(T, H) = \partial M(T, H)/\partial H$ could readily be obtained. In

Fig.8 (top) some of the resulting susceptibility curves are shown for selected values of H . The experimental $H(T_{max})$ is plotted at the bottom of Fig.8. This graph, in contrast to the one of the “pure” 2D Ising model, shows two distinct regimes, depending on the range of H . We discuss first the low temperature regime. When cooling in weak enough fields, the system first enters the “gray zone”, (see the phase diagram in Fig.2 of the main document), without displaying any anomaly in the susceptibility in correspondence of this transition. Upon further cooling a re-entrant transition from the patterned to the uniform phase is encountered^{17,18,38}: this second transition is accompanied by a sharp maximum in the susceptibility (abrupt increase of the magnetization). This type of maxima – highlighted by a blue dashed line in Fig.8 (bottom) – when extrapolated to $H = 0$ leads to a temperature at which the sample consists of very large stripes carrying opposite but almost saturated values of the magnetization^{17,18,38}. Above this temperature, the sample keeps the modulated order up T^* , where domains become mobile but the magnetization within them is still substantial. Accordingly, T_C must be above T^* . On the other side, for larger fields (the right-hand side portion of the graph) the “gray zone” is never entered and the system is in a uniform state: $H(T_{max})$ for larger H was therefore taken to extrapolate towards a putative T_C . Several linear fittings were performed by choosing different ranges of the field $\mu_0 \cdot H$ between $30 \cdot 10^{-4}$ T and $80 \cdot 10^{-4}$ T. The different fittings produced the family of red lines (bottom of Fig.8) from which the error on the T_C was estimated. The experimental T_C , for this particular sample, is 300 ± 1 K. Notice that the extrapolated T_C lies within the cross-over range (K) $298 \lesssim T \lesssim 302$, in which the “blue-line” types of maxima transform into the “red-line” types of maxima.

Appendix B: Experimental determination of β and δ

The critical exponent β can be deduced from the experimentally determined values of the exponents γ and δ , using the relation $\beta\delta = \beta + \gamma$. The exponent γ determines the magnetization in the region of weak fields (Eq. 148.8. in Ref. 1) according to

$$M \sim \frac{H}{|\tau|^\gamma}. \quad (\text{B1})$$

The exponent δ determines the magnetization in the region of strong fields according to the relation

$$M \sim H^{1/\delta} \quad (\text{B2})$$

(see Eq. 148.10 in Ref. 1). The notion of “weak” and “strong” field is, of course, dependent on which temperature interval is addressed.

In Fig.9 we plot $\log(M/H)$ versus $\log |\tau|$ for different values of H , with the color code indicating the values of H (see horizontal scale in the inset). At sufficiently high

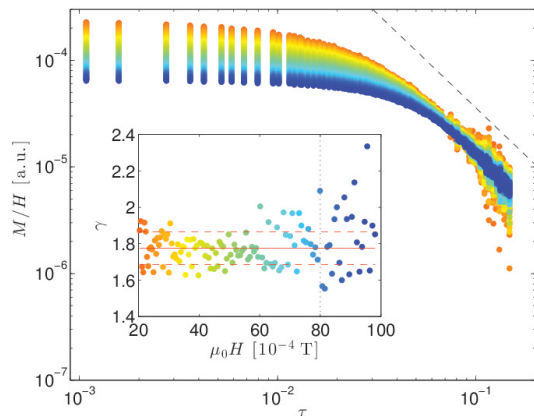


FIG. 9: Log-log plot of the ratio M/H vs $\tau = (T - T_C)/T_C$ (with $T_C = 300$ K); the dashed black line is a guide to the eye with slope equal to the mean value of γ . Different isochoamps are plotted with different colors; specific values of the field H can be identified from the horizontal axis of the inset, where fitted values of γ obtained for different fields are plotted (see the text); the solid and dashed horizontal lines indicate the mean value of γ and the standard deviation from this average, respectively; the vertical dotted line marks the largest field $\mu_0 \cdot H = 80 \cdot 10^{-4}$ T used to determine γ .

temperatures, a region of the graph emerges where all curves for different magnetic fields almost collapse onto one single straight line, and thus fulfill the scaling properties required by Eq. (1) for the quantity M/H . The negative of the slope of the resulting straight line is the sought-for exponent γ . Several linear fittings were performed for fixed fields ranging from $20 \cdot 10^{-4}$ T to $80 \cdot 10^{-4}$ T; these independent determinations of γ are shown in the inset. After averaging, for $T_C = 300$ K we obtain

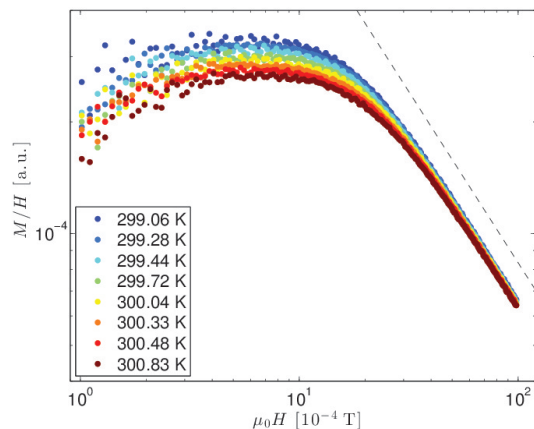


FIG. 10: Log-log plot of the ratio M/H vs H . Different isotherms are plotted with different colors (specific values of T are given in the legend). The dashed black line is a guide to the eye with slope equal to mean value of $(1 - \delta)/\delta$ (fitted exponents).

$\gamma = 1.78 \pm 0.09$, with the error given by the standard deviation of the mean. As consistency check, the whole procedure was repeated varying the value of T_C . The standard deviation of the mean values of γ goes through a minimum in the range (K) $298 \leq T_C \leq 301$, which is, accordingly, the range where the “best collapsing” of the M/H -curves is realized. When T_C is varied in this interval, γ ranges from 1.7 to 1.9.

The $\log(M/H)$ versus $\log H$ plot of Fig.10 in the temperature range (K) $299 < T < 301$, reveals a low-field region where the curves saturate to an almost constant value, indicating the linearity of M versus H for weak fields. In the strong-field region the graphs are observed to almost collapse onto a single straight line, the slope of which amounts to $(1 - \delta)/\delta$, consistently with Eq. 2. From these slopes fitted for different T in the appropriate regime of Fig.10 we estimate $\delta = 13 \pm 2$.

- * Electronic address: vindigni@phys.ethz.ch
- ¹ Landau, L.D., Lifshitz, E.M., *Statistical Physics*, Vol.5 of Course of Theoretical Physics, Pergamon Press Ltd., Oxford, Third Revised and Enlarged Edition 1980, p.483-493
 - ² The lack of uniform magnetization in finite three dimensional bodies appears to be a necessary consequence of a theorem by Griffiths R.B., (1968), Free Energy of interacting magnetic dipoles, *Phys. Rev.* 176, 655-659, as pointed out e.g. in Ref. 3 and Ref. 4
 - ³ Arrott A, (1968), Existence of a critical line in ferromagnetic to paramagnetic transitions, *Phys. Rev. Lett.* 20, 1029-1031
 - ⁴ Bramwell ST, (2010), Dipolar effects in condensed matter, in "Long Range Interacting Systems", Edited by T. Dauxois, S. Ruffo and L.F. Cugliandolo, Oxford University Press, Oxford, UK
 - ⁵ Kivelson D, Kivelson SA, Zhao X, Nussinov Z, Tarjus G, (1995), A thermodynamic theory of supercooled liquids, *Physica A* 219, 27-38
 - ⁶ Brazovskii SA, (1975), Phase transitions of an isotropic system to a nonuniform state, *Sov. Phys. JETP* 41, 85-89
 - ⁷ Abanov Ar, Kalatsky V, Pokrovsky VL and Saslow WM, (1995), Phase diagram of ultrathin ferromagnetic films with perpendicular anisotropy, *Phys. Rev. B* 51, 1023-1038
 - ⁸ Barci DG, Stariolo DA, (2009) Orientational order in two dimensions from competing interactions at different scales, *Phys. Rev. B* 79, 075437(6)
 - ⁹ Cannas SA, Stariolo DA, Tamarit FA, (2004), Stripe-tetragonal first-order phase transition in ultrathin magnetic films, *Phys. Rev. B* 69, 092409(4)
 - ¹⁰ Schmalian J, Wolynes PG, (2000), Stripe Glasses: Self-Generated Randomness in a Uniformly Frustrated System, *Phys. Rev. Lett.* 85, 836-839
 - ¹¹ See also Tarjus G, Kivelson SA, Nussinov Z, Viot P, (2005), The frustration-based approach of supercooled liquids and the glass transition: a review and critical assessment *J. Phys.: Condens. Matter* 17, R1143-R1182 (2005) and references therein for a general review of theoretical results on the phase transition in systems frustrated by long-ranged interactions.
 - ¹² Saratz N,(2010),Inverse Symmetry Breaking in Low-Dimensional Systems, Logos Verlag GmbH, Berlin
 - ¹³ Onsager L, (1944), Crystal Statistics. I. A Two-Dimensional Model with an Order-Disorder Transition, *Phys. Rev.* 65, 117-149
 - ¹⁴ Biskup M, Chayes L, Kivelson SA, (2007), On the Absence of Ferromagnetism in Typical 2D Ferromagnets, *Comm. Math. Phys.* 274, 217-321
 - ¹⁵ See Seul M, Andelman D, (1995), Domain Shapes and Patterns: The Phenomenology of Modulated Phases, *Science* 267, 476-483 for a review on systems with modulated order.
 - ¹⁶ Allenspach R, Bischof A, (1992),Magnetization direction switching in Fe/Cu(100) epitaxial films: Temperature and thickness dependence, *Phys. Rev. Lett.* 69, 3385-3388
 - ¹⁷ Saratz N, Lichtenberger A, Portmann O, Ramsperger U, Vindigni A, Pescia D,(2010) Experimental Phase Diagram of Perpendicularly Magnetized Ultrathin Ferromagnetic Films, *Phys. Rev. Lett.* 104 077203(4)
 - ¹⁸ Saratz N, Ramsperger U, Vindigni A, Pescia D, (2010) Irreversibility, reversibility, and thermal equilibrium in domain patterns of Fe films with perpendicular magnetization, *Phys. Rev. B* 82, 184416(11) and references therein.
 - ¹⁹ Chen G, Zhu J, Quesada A, Li J, Diaye ATN, Huo Y, Ma TP, Chen Y, Kwon HJ, Won C, Qiu ZQ, Schmid AK, Wu YZ, (2013) Novel Chiral Magnetic Domain Wall Structure in Fe/Ni/Cu(001) Films, *Phys. Rev. Lett.* 110, 177204(5)
 - ²⁰ Kronseder M, Buchner M, Bauer HG, Back CH, (2013) Dipolar-energy-activated magnetic domain pattern transformation driven by thermal fluctuations, *Nat. Commun.* 4:2054, doi: 10.1038/ncomms3054
 - ²¹ Cannas SA, Carubelli M, Billoni OV, Stariolo DA, (2011), Inverse transition in a two-dimensional dipolar frustrated ferromagnet, *Phys. Rev. B* 84, 014404(7)
 - ²² De'Bell K, MacIsaac AB, Whitehead JP, (2000) Dipolar effects in magnetic thin films and quasi-two-dimensional systems *Rev. Mod. Phys.* 72, 225-257
 - ²³ Diaz-Mendez R, Mulet R, (2010) H-T phase diagram of the two-dimensional Ising model with exchange and dipolar interactions *Phys. Rev. B* 81, 184420(9); Rastelli E, Regina S, Tassi A, (2007) Phase diagram of a square Ising model with exchange and dipole interactions: Monte Carlo simulations *Phys. Rev. B* 76, 054438(22)
 - ²⁴ Pighin SA, Cannas SA, (2007) Phase diagram of an Ising model for ultrathin magnetic films: Comparing mean field and Monte Carlo predictions, *Phys. Rev. B* 75, 224433(9)
 - ²⁵ Liu C, Moog ER, Bader SD, (1988) Polar Kerr-Effect Observation of Perpendicular Surface Anisotropy for Ultrathin fcc Fe Grown on Cu(100), *Phys. Rev. Lett.* 60, 2422-2425
 - ²⁶ Portmann O, Vaterlaus A, Pescia D, (2006) Observation of Stripe Mobility in a Dipolar Frustrated Ferromagnet, *Phys. Rev. Lett.* 96, 047212(4)
 - ²⁷ Gaunt DS, Domb C, (1970) Equation of state of the Ising model near the critical point *J. Phys. C: Solid St. Phys* 3, 1442-1461
 - ²⁸ Cannas SA, Michelon MF, Stariolo DA Tamarit FA, (2006) Ising nematic phase in ultrathin magnetic films: A Monte Carlo study, *Phys. Rev. B* 73, 184425(12)
 - ²⁹ On one side, the necessity of summing over *all* pairs, imposed by the presence of the dipolar interaction, limits the size of the system for realistic simulation times to about $L_x = L_y = 200$. On the other side, the width of domains increases exponentially with J/g : In order to observe domain phases within the given L_x the ratio J/g cannot be as large as in the experiment, where $T_C/g \sim O(10^2)$.
 - ³⁰ After having prepared the system in a uniform saturated state (with $m = 1$), we let the temperature increase from very low values up to a predefined T_f , lying above the transition from the modulated to the paramagnetic phase for $h = 0$. Then, we stopped the simulation and, starting from the final configuration, the system was cooled down to the original temperature. When $h < h_c$ a strong hysteresis in the $m(T)$ curves was observed, below the temperature where modulated phases develop. When $h > h_c$, instead, the curves were completely reversible in the whole temperature range. In this way we could estimate h_c for rather large values of J/g (up to $J/g = 10$), without the computational cost of complete phase-diagram calculations.
 - ³¹ Griffiths RB, (1966) Spontaneous Magnetization in idealized Ferromagnets, *Phys. Rev.* 152, 240-246
 - ³² For a concise summary of the earlier results on phase transitions in the presence of the dipolar interaction see e.g.

- Pokrovskii VL, (2013) Works by A.I. Larkin on the theory of phase transitions *J. Exp. Theo. Phys.* 117, 387-391 and the references quoted therein
- ³³ Fisher ME, Aharony A, (1973) Dipolar Interactions at ferromagnetic critical points, *Phys. Rev. Lett.* 30, 559-562
- ³⁴ Our results have shown that the size of domains can change from few 100 μm to few 10 nm within a narrow temperature range in the transition region, so that a state which appear to be uniform sufficiently below T_C cannot be automatically assumed to remain uniform when the transition temperature is approached.
- ³⁵ Accordingly, the numerous literature (which cannot be quoted exhaustively for obvious reasons) reporting the quantitative determination of critical properties contains inevitably (conscious or unconscious) assumptions on the set of data used for the quantitative determination of – say – critical exponents. A. Aharoni, Introduction to the theory of ferromagnetism, Clarendon Press, Oxford, 1996, p.68 goes as far as stating that “...the data can be fitted to almost any value of the critical exponent...” and later “Some of the critical exponents may be more reliable when they are obtained from the analogy with other critical phenomena that do not have the equivalent of a magnetic field and magnetic domains.”
- ³⁶ Chang KJ, Lee KC, (1980), The critical behaviour of the maximum susceptibility locus *J. Phys. C: Solid State Phys.* 13, 2165-2170
- ³⁷ Onsager L, (1944), Crystal Statistics. I. A Two-Dimensional Model with an Order-Disorder Transition, *Phys. Rev.* 65, 117-149
- ³⁸ Portmann O, Gölzer A, Saratz N, Billoni OV, Pescia D, Vindigni A, (2010) Scaling hypothesis for modulated systems, *Phys. Rev. B* 82, 184409(13)
- ³⁹ Griffiths RB, (1967), Thermodynamic Functions for Fluids and Ferromagnets near the Critical Point, *Phys. Rev.* 158, 176-187
- ⁴⁰ Use Eq.16 in Ref. 38 and Eq.2.20, 2.38 in Ref. 12